National Conference with International Participation
ENGINEERING MECHANICS 2007
Svratka, Czech Republic, May 14 – 17, 2007

SUPPRESSION OF THE SELF-EXCITED VIBRATION OF THE PENDULUM SYSTEM INDUCED BY FLOW

Radoslav NABERGOJ(*) and Aleš TONDL(**)

(*) Dept. of Naval Architecture, Ocean and Environmental Engineering, Via Valerio 10, 34127 Trieste, Italy
(**) Zborovska 41, Prague 5, CZ-150 00 Czech Republic

1. INTRODUCTION

In [1, 2] the effect of two absorbers for quenching self-excited vibrations induced by flow is treated. In the first case the absorber can move perpendicularly, while in the second one along the axis of the pendulum. Thus the arrangement of the absorber mass differs substantially.

In this contribution a pendulum system as in Figure 1 is treated. Here, not only the absorber damping effect is considered but also his application as an active tool for vibration suppression through parametric excitation. The parametric excitation is due to periodic stiffness variation of the elastic mounting of absorber mass. The positive effect of parametric excitation for suppressing self-excited vibration was discovered when analyzing interaction of self-excitation and parametric excitation [3], while the conditions for a full suppression self-excited vibration were formulated later on, see [4, 5].

The basic pendulum system in Figure 1 is characterized by the concentrated mass M at distance l from the pendulum suspension point O and by the absorber of mass m located at a distance l_0 from M. The distance of the absorber mass m from the pendulum axis is $(l+l_0)\tan(\psi-\varphi)$, where φ, ψ are the deflection angles with respect to the vertical direction. For small values of φ and ψ it can be assumed that $(l+l_0)\tan(\psi-\varphi)\approx(l+l_0)(\psi-\varphi)$. This relation would be perfectly true in case of a circular trajectory of the absorber's mass.

2. DIFFERENTIAL EQUATIONS OF MOTION

The self-excitation due to the flow can be modeled by van der Pol terms. We assume that for the case of a passive tool the stiffness of the absorber spring k remains constant while for the case of an active tool using parametric excitation it varies in time according to the relation $k(t)=k_0(1+\varepsilon\cos\omega t)$. This stiffness variation can be established, e.g., by a controlled magnetic force acting on the absorber's mass.

Considering the kinetic (K) and potential (U) energies, one has:

$$T=\frac{1}{2}Ml^2\dot{\varphi}^2+\frac{1}{2}m(l+l_0)^2\dot{\psi}^2\ , \tag{1}$$

$$U=\frac{1}{2}Mgl(1-\cos\varphi)+\frac{1}{2}mg(l+l_0)(1-\cos\psi)+\frac{1}{2}k(l+l_0)^2(\psi-\varphi)^2\ . \tag{2}$$

Thus, by assuming the van der Pol model for self-excitation and a linear viscous damping for the absorber, the above system is governed by the following differential equations of motion:

$$Ml^2\ddot{\varphi}-\left(b-d\varphi^2\right)\dot{\varphi}+Mgl\sin\varphi-b_0\left(\dot{\psi}-\dot{\varphi}\right)-k\left(l+l_0\right)^2\left(\psi-\varphi\right)=0\,,$$
$$m\left(l+l_0\right)^2\ddot{\psi}+mg\left(l+l_0\right)\sin\psi+b_0\left(\dot{\psi}-\dot{\varphi}\right)+k\left(l+l_0\right)^2\left(\psi-\varphi\right)=0\,. \tag{3}$$

Thus, after proper rearrangement of equations (3) we obtain the form:

$$\ddot{\varphi}-\left(\frac{b}{Ml^2}-\frac{d}{Ml^2}\varphi^2\right)\dot{\varphi}+\frac{g}{l}\sin\varphi-\frac{b_0}{Ml^2}\left(\dot{\psi}-\dot{\varphi}\right)-\frac{k\left(l+l_0\right)^2}{Ml^2}\left(\psi-\varphi\right)=0\,,$$
$$\ddot{\psi}+\frac{g}{l+l_0}\sin\psi+\frac{b_0}{m\left(l+l_0\right)^2}\left(\dot{\psi}-\dot{\varphi}\right)+\frac{k}{m}\left(\psi-\varphi\right)=0\,. \tag{4}$$

By using the time transformation

$$\tau=\omega_0 t\,,\quad \omega_0=\sqrt{\frac{g}{l}}\;, \tag{5}$$

and assuming that small oscillations will occur, equations (4) get the form:

$$\varphi''-\left(\beta-\delta\varphi^2\right)\varphi'+\varphi-\frac{\kappa\mu}{\alpha^2}\left(\psi'-\varphi'\right)-\frac{\mu q^2}{\alpha^2}\left(\psi-\varphi\right)=0\,,$$
$$\psi''+\alpha\psi+\kappa\left(\psi'-\varphi'\right)+q^2\left(\psi-\varphi\right)=0\,, \tag{6}$$

where:

$$\mu=\frac{m}{M}\,,\quad q^2=\frac{k}{m\omega_0^2}=\frac{kl}{mg}\,,\quad \alpha=\frac{g}{\left(l+l_0\right)\omega_0^2}=\frac{l}{l+l_0}\,,\quad \beta=\frac{b}{Ml^2\omega_0}\,,\quad \delta=\frac{d}{Ml^2\omega_0}\,,$$
$$\kappa=\frac{b_0}{m\left(l+l_0\right)^2\omega_0}\,,\quad q^2=q_0^2\left(1+\varepsilon\cos\eta\tau\right),\quad \eta=\omega/\omega_0\,.$$

Assuming that the damping coefficients and the amplitude ε are small, the abbreviated system reads:

$$\varphi''+\left(1+\frac{\mu q_0^2}{\alpha^2}\right)\varphi-\frac{\mu q_0^2}{\alpha^2}\psi=0\,,$$
$$\psi''+\left(\alpha+q_0^2\right)\psi-q_0^2\varphi=0\,. \tag{7}$$

The natural frequencies can be determined from the equation:

$$\begin{vmatrix}1+\dfrac{\mu q_0^2}{\alpha^2}-\Omega^2 & -\dfrac{\mu q_0^2}{\alpha^2}\\ -q_0^2 & \alpha+q_0^2-\Omega^2\end{vmatrix}=\Omega^4-\left[1+\alpha+q_0^2\left(1+\frac{\mu}{\alpha^2}\right)\right]\Omega^2+\left(1+\frac{\mu q_0^2}{\alpha^2}\right)\left(\alpha+q_0^2\right)-\frac{\mu q_0^4}{\alpha^2}=0\,. \tag{8}$$

Hence, using transformation:

$$\varphi=y_1+y_2\,,$$
$$\psi=a_1y_1+a_2y_2\,, \tag{9}$$

where:

$$a_j=\frac{q_0^2}{\alpha+q_0^2-\Omega_j^2}\,,\quad (j=1,2)\,.$$

equations (6) can be transformed into the quasi-normal form:

$$y_s''+\Omega_s^2y_s+\sum_{k=1}^{2}\left(\Theta_{sk}y_k'+Q_{sk}\cos\eta\tau\right)=0\,,\quad \left(s=1,2\right). \tag{10}$$

For system (10) the coefficients are:

$$
\begin{aligned}
\Theta_{11} &= \frac{1}{a_1 - a_2}\left[\beta a_2 - \kappa(1-a_1)\left(1 + a_2\frac{\mu}{\alpha^2}\right)\right],\\
\Theta_{12} &= \frac{1}{a_1 - a_2}\left[\beta a_2 - \kappa(1-a_2)\left(1 + a_2\frac{\mu}{\alpha^2}\right)\right],\\
\Theta_{21} &= \frac{1}{a_1 - a_2}\left[-\beta a_1 + \kappa(1-a_1)\left(1 + a_1\frac{\mu}{\alpha^2}\right)\right],\\
\Theta_{22} &= \frac{1}{a_1 - a_2}\left[-\beta a_1 + \kappa(1-a_2)\left(1 + a_1\frac{\mu}{\alpha^2}\right)\right],\\
Q_{11} &= -\frac{\varepsilon q_0^2}{a_1 - a_2}(1-a_1)\left(1 + a_2\frac{\mu}{\alpha^2}\right),\\
Q_{12} &= -\frac{\varepsilon q_0^2}{a_1 - a_2}(1-a_2)\left(1 + a_2\frac{\mu}{\alpha^2}\right),\\
Q_{21} &= \frac{\varepsilon q_0^2}{a_1 - a_2}(1-a_1)\left(1 + a_1\frac{\mu}{\alpha^2}\right),\\
Q_{22} &= \frac{\varepsilon q_0^2}{a_1 - a_2}(1-a_2)\left(1 + a_1\frac{\mu}{\alpha^2}\right).
\end{aligned}
\tag{11}
$$

When $\Theta_{jj} < 0$, $(j = 1,2)$ the corresponding vibration mode can be initiated. However, if all $\Theta_{jj} > 0$ then the equilibrium position is stable.

The parametric excitation can stabilize the equilibrium position at the combination frequency $\eta \approx \eta_0 = \Omega_2 - \Omega_1$ (see [3, 4]) if the following conditions are met:

$$\Theta_{11} + \Theta_{22} > 0, \tag{12}$$

$$\frac{Q_{12}Q_{21}}{4\Omega_1\Omega_2} + \Theta_{11}\Theta_{22} > 0. \tag{13}$$

When inserting Θ_{11}, Θ_{22} from (11), condition (12) gets the form:

$$-\beta + \left(1 + \frac{\mu}{\alpha^2}\right)\kappa > 0. \tag{14}$$

Moreover, inserting Θ_{11}, Θ_{22}, Ω_1, Ω_2, Q_{12}, Q_{21}, in condition (13) we obtain:

$$\varepsilon^2 > \frac{4\Omega_1\Omega_2\left[-\beta a_1 + \kappa(1-a_1)\left(1 + a_1\frac{\mu}{\alpha^2}\right)\right]\left[\beta a_2 - \kappa(1-a_2)\left(1 + a_2\frac{\mu}{\alpha^2}\right)\right]}{q_0^4(1-a_1)(1-a_2)\left(1 + a_1\frac{\mu}{\alpha^2}\right)\left(1 + a_2\frac{\mu}{\alpha^2}\right)}. \tag{15}$$

Equation (15) allows one to determine the boundary value of the parametric excitation for which the equilibrium position is stable at frequency $\eta \approx \eta_0 = \Omega_2 - \Omega_1$. When $\varepsilon^2 < 0$, i.e. $\Theta_{11}\Theta_{22} > 0$, one has that the equilibrium position is stable even if parametric excitation is not applied. Thus, the boundary value ε_B can be obtained from (15) by satisfying the condition $\varepsilon_B^2 = 0$.

The calculation of the boundary value ε_B for different system parameters enables one to optimize the design parameters of the absorber, first of all the location α and the tuning q_0, the remaining parameters being assigned. Here we can stress some difficulties for practical applications: the first one is related to the limitations of the absorber mass, while the second one requires that the distance of the absorber from the center of gravity of the basic pendulum system cannot be excessive.

3. EXAMPLES

The stability of system (6) has been investigated by searching for the normal mode frequencies (8) and by solving equation (15) to obtain the boundary values ε_B for the parametric excitation. Thus in Figures 2-7 we show the boundary values of parametric excitation necessary for the suppression of self-excited vibrations together with the normal mode frequencies Ω_1 and Ω_2, and the combination frequency $\eta_0 = \Omega_2 - \Omega_1$. The results in Figures 2-4 highlight the effect of α and refer to $\mu = 0.05$, $\beta = \kappa = 0.05$ and different values of q_0^2, which are ranging from 0.20 to 0.80. It can be seen that reasonable values for parametric excitation boundary can be obtained for $\alpha < 1$, i.e. for $l < l + l_0$. This implies $l_0 > 0$, i.e., the self-excited vibration can be damped only when the weight is located below the centre of mass of the pendulum. Moreover, in Figure 2 the boundary value ε_B clearly indicates that there exists a broad interval of α (0.05< α <0.29) where both Θ_{11} and Θ_{22} are positive and parametric excitation is not necessary to suppress the vibration. Taking into account that a system with the absorber far from the center of gravity can hardly be build, it is important to consider the boundary $\varepsilon_B(\alpha)$ in the proximity of α = 0.78 for which the absorber can easily be designed.

The effect of mass ratio μ is shown in Figure 5, while Figure 6 shows the effect of the tuning q_0^2. It can be seen that parametric excitation is able to suppress self-excited vibrations for $q_0^2 \approx 0.23$, while the optimal mass values are around $\mu = 0.01$.

Figure #	μ	q_0^2	α	κ	β	δ	ε	η
7	0.01	0.80	0.30	0.10	0.10	2.00	0.30	variable
8	0.05	0.80	0.30	0.10	0.10	0.40	0.30	variable
9	0.05	0.40	0.60	0.10	0.10	0.40	0.30	variable
10	0.05	0.80	0.30	0.10	0.10	0.40	0.30	0.55
11	0.05	0.228	0.75	0.05	0.05	0.40	0.50	0.0713

Table 1 – Values of system parameters for numerical simulation.

The parameter values of the examples considered are shown in Table 1. Figures 7, 8 and 9 show the extreme deflections of quasi-normal coordinates as a function of η. As expected, a significant reduction of vibration amplitude for both $[\varphi]$ and $[\psi]$ occurs in both figures for $\eta \simeq \eta_0 = \Omega_2 - \Omega_1$, where the parametric excitation is able to suppress self-excited vibrations at the combination frequency. The amplitude remains almost constant in the whole frequency range, but an amplitude increase is observed at the subharmonic resonance $\eta \simeq 2\Omega_1$ and the combination resonance $\eta \simeq \Omega_1 + \Omega_2$.

In Figure 10 we show an example of time domain simulation where the efficiency of suppressing self-excited vibrations by means of parametric excitation is clearly demonstrated. The same is not true for the example of Figure 11, even if the system parameters and the excitation have been properly selected. This opens the problem of further analysis which is necessary to better understand the limits of the suppression process.

CONCLUSIONS

The presented analysis proves that an absorber subsystem added to the basic pendulum system can suppress self-excited vibration due to negative linear damping component (e.g. the one generated by the action of the flow) especially when using parametric excitation due to stiffness variation of the elastic mounting of the absorber mass. Here the phenomenon of parametric anti-resonance is highlighted. The results of the theoretical analysis, supplemented by numerical simulations, give the basis for finding the optimal tuning of the absorber subsystem. The suppressing efficiency is influenced both by the tuning of the absorber as well as by its location in the system.

REFERENCES

[1] Nabergoj R., Springer H. and Tondl A.: Two dynamic absorbers for quenching self-excited vibration of a pendulum, Proc. International Conference Engineering Mechanics 2000, Svratka, , 2000, Editors: J. Naprstek and J. Minster, Vol. II, pp. 9-16.
[2] Tondl A., Kotek V. and Kratochvil C.: Vibration quenching of pendulum type systems by means of absorbers, CERM akad. nakl. s.r.o., Brno, 2001.
[3] Tondl A.: On the Interaction between self-excited and parametric vibrations. Monographs and Memoranda, No. 25, National Research Institute for Machine Design, Prague, 1978.
[4] Tondl A.: To the problem of quenching self-excited vibrations. Acta Technica CSAV 43, pp. 109-116, 1998.
[5] Ecker H.: Suppression of self-excited vibrations in mechanical systems by parametric stiffness excitation. Fortschrifttsberichte Simulation, Band 11, ARGESIM/ASIM-Verlag, Wien, 2003.

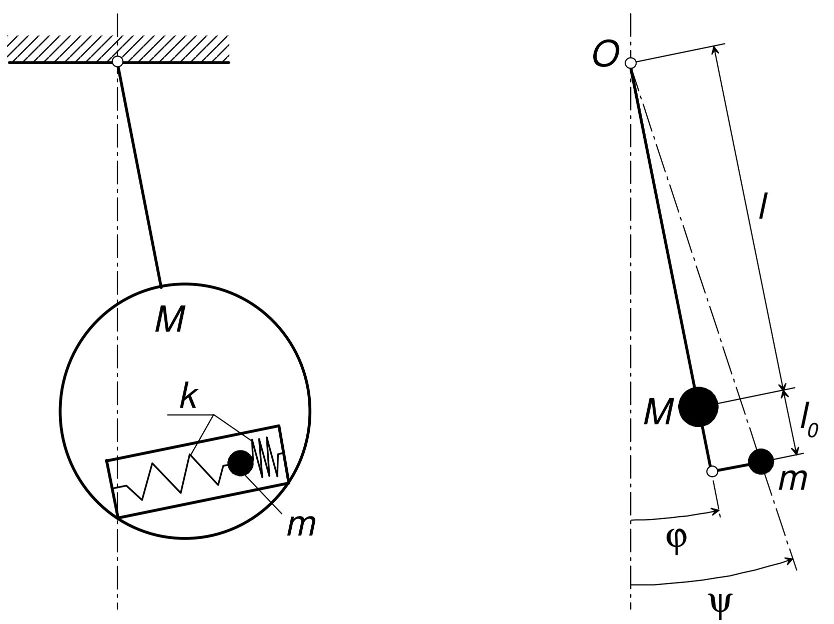

Figure 1- Schematic representation of the model.

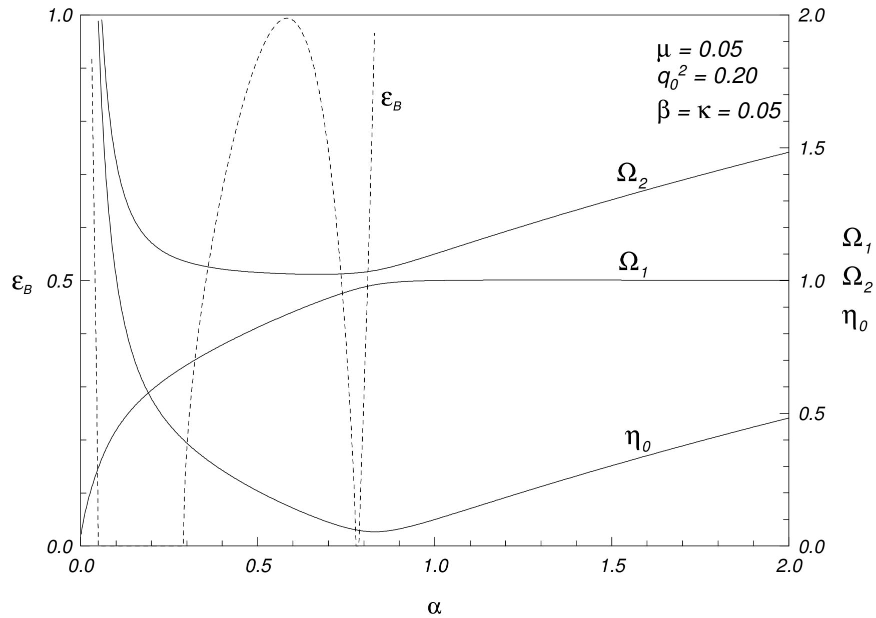

Figure 2 – Parametric excitation limit ε_B as a function of α for $\mu = 0.05$, $q_0^2 = 0.20$, $\beta = \kappa = 0.05$, together with the normal mode frequencies Ω_1, Ω_2, and the combination frequency $\eta_0 = \Omega_2 - \Omega_1$.

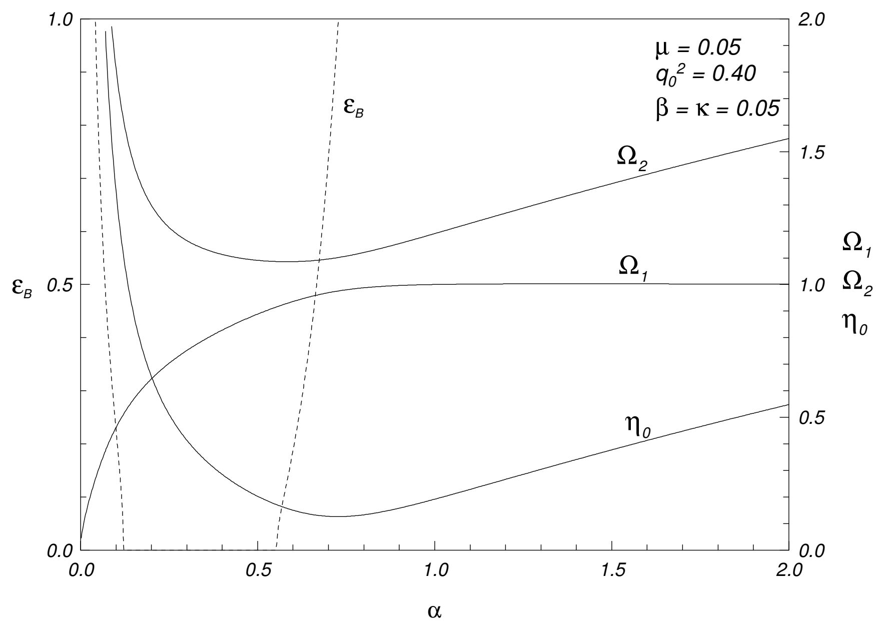

Figure 3 – Parametric excitation limit ε_B as a function of α for $\mu = 0.05$, $q_0^2 = 0.40$, $\beta = \kappa = 0.05$, together with the normal mode frequencies Ω_1, Ω_2, and the combination frequency $\eta_0 = \Omega_2 - \Omega_1$.

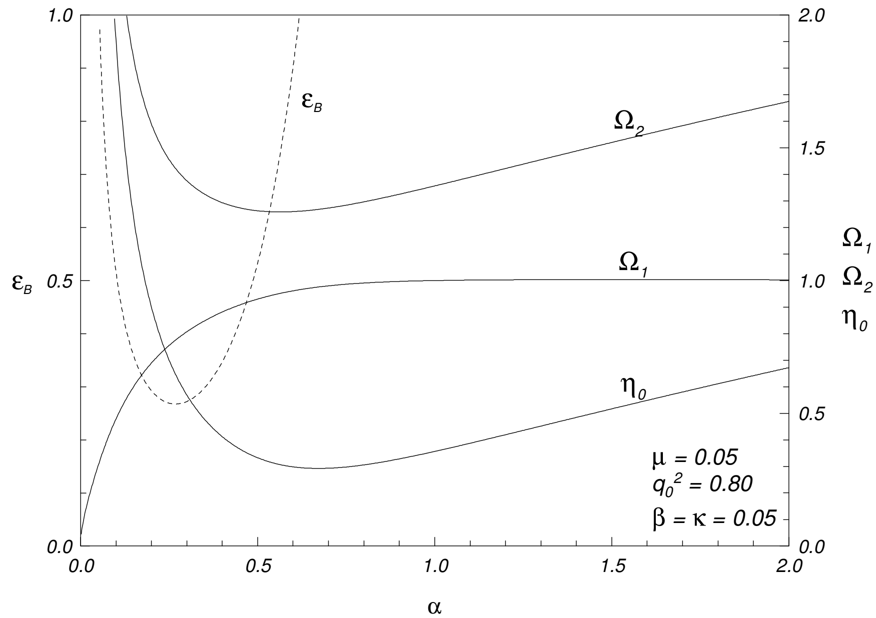

Figure 4 – Parametric excitation limit ε_B as a function of α for $\mu = 0.05$, $q_0^2 = 0.80$, $\beta = \kappa = 0.05$, together with the normal mode frequencies Ω_1, Ω_2, and the combination frequency $\eta_0 = \Omega_2 - \Omega_1$.

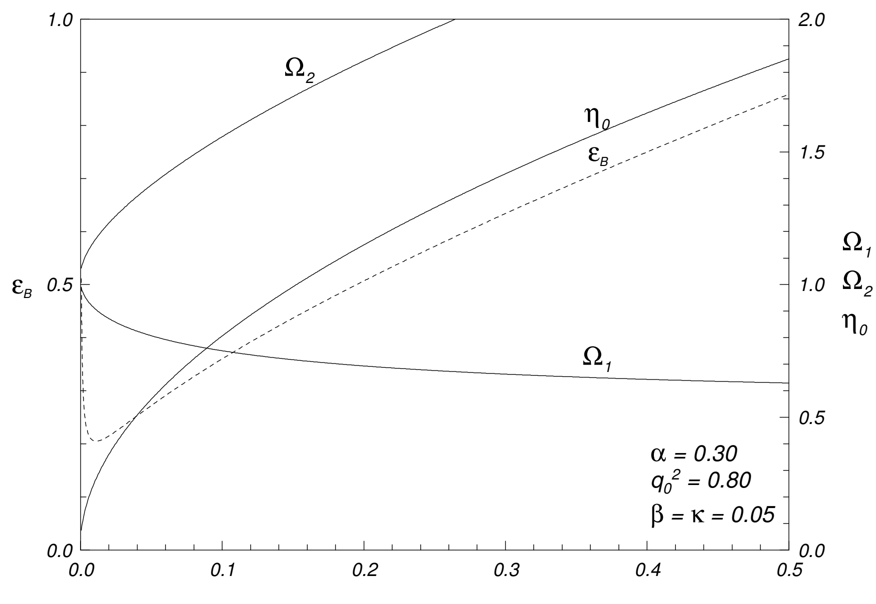

Figure 5 – Parametric excitation limit ε_B as a function of μ for $\alpha = 0.30$, $q_0^2 = 0.80$, $\beta = \kappa = 0.05$, together with the normal mode frequencies Ω_1, Ω_2, and the combination frequency $\eta_0 = \Omega_2 - \Omega_1$.

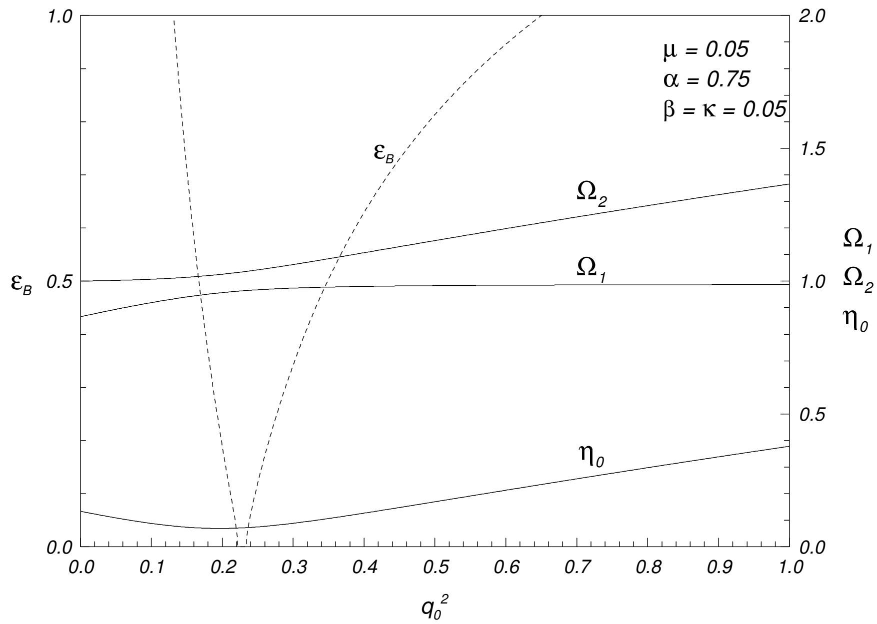

Figure 6 – Parametric excitation limit ε_B as a function of q_0^2 for $\mu = 0.05$, $\alpha = 0.75$, $\beta = \kappa = 0.05$, together with the normal mode frequencies Ω_1, Ω_2, and the combination frequency $\eta_0 = \Omega_2 - \Omega_1$.

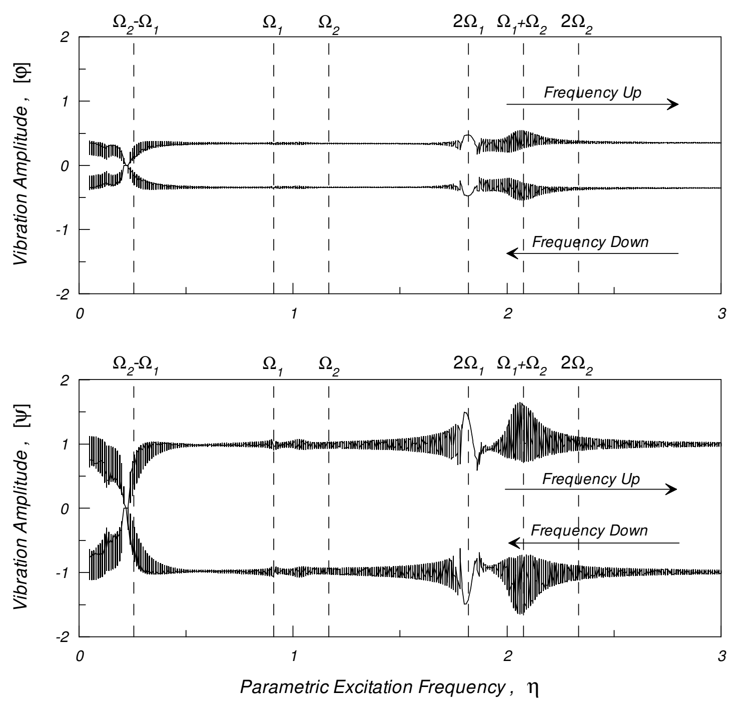

Figure 7 – Extreme values $[\varphi]$ and $[\psi]$ of system vibration amplitudes φ and ψ versus applied parametric excitation frequency η for μ =0.01, q_0^2 = 0.80, $\alpha = 0.30$, $\kappa = 0.10$, $\beta = 0.10$, $\delta = 2.00$, and $\varepsilon = 0.30$.

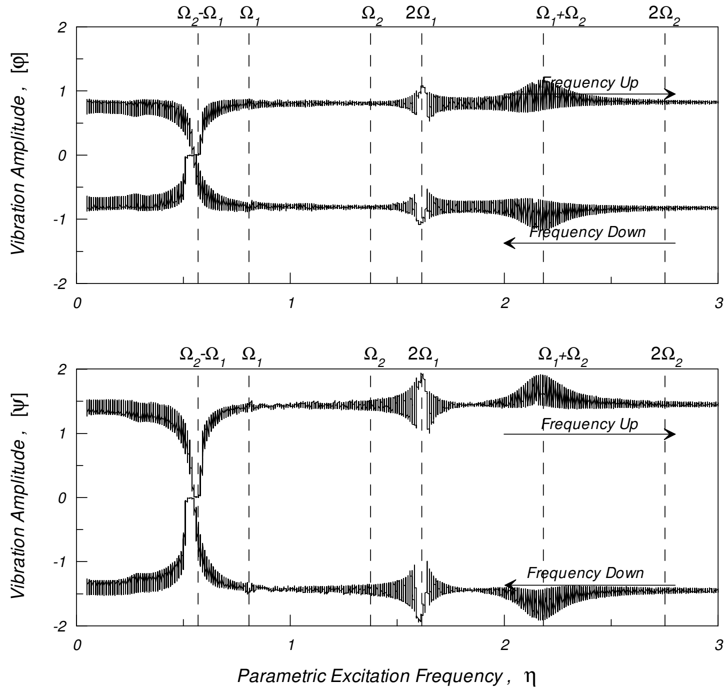

Figure 8 – Extreme values $[\varphi]$ and $[\psi]$ of system vibration amplitudes φ and ψ versus applied parametric excitation frequency η for μ =0.05, q_0^2 = 0.80, $\alpha = 0.30$, $\kappa = 0.10$, $\beta = 0.10$, $\delta = 0.40$, and $\varepsilon = 0.30$.

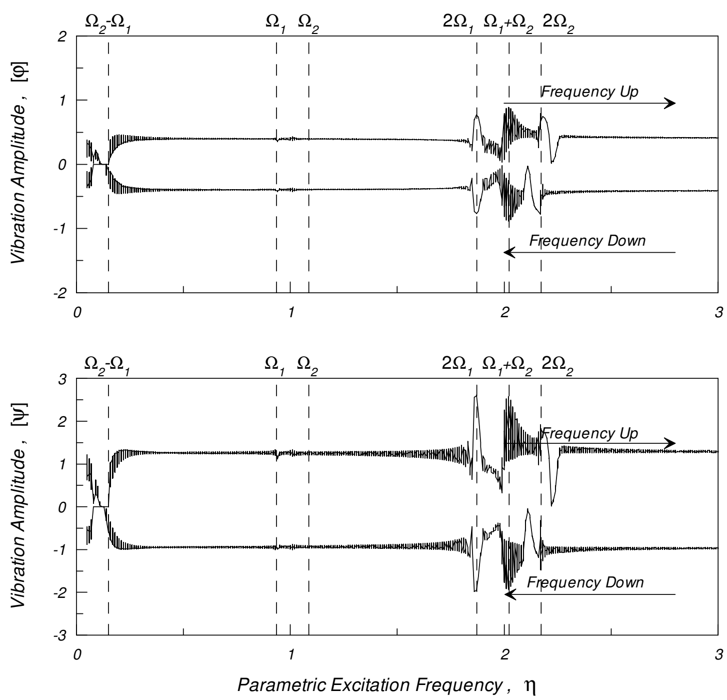

Figure 9 – Extreme values $[\varphi]$ and $[\psi]$ of system vibration amplitudes φ and ψ versus applied parametric excitation frequency η for μ =0.01, q_0^2 = 0.40, $\alpha = 0.60$, $\kappa = 0.10$, $\beta = 0.10$, $\delta = 2.00$, and $\varepsilon = 0.30$.

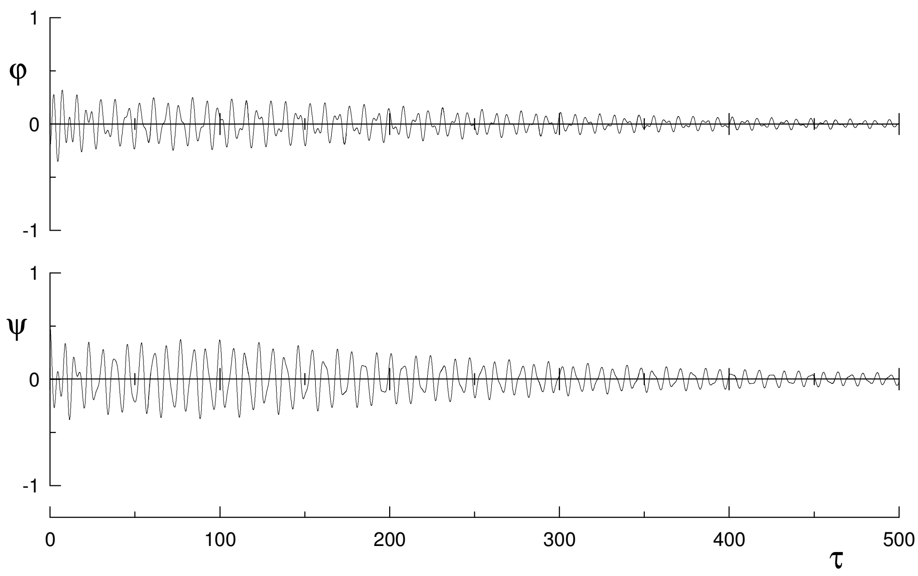

Figure 10 – Time domain simulation for μ =0.05, q_0^2 = 0.80, α = 0.30, κ = 0.10, β = 0.10, δ = 0.40, ε = 0.30 and η = 0.55, where the efficiency of suppressing self-excited vibration is shown.

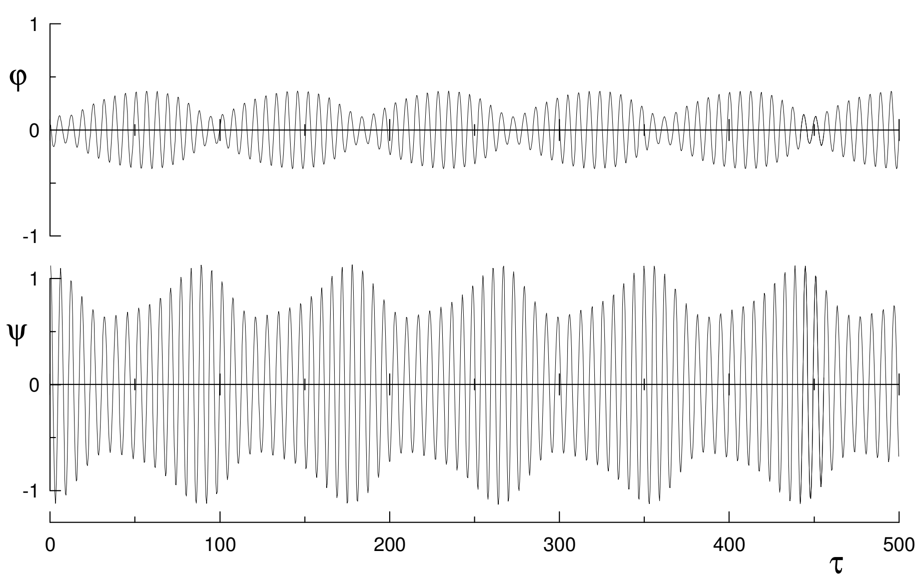

Figure 11 – Time domain simulation for μ =0.05, q_0^2 = 0.80, α = 0.75, κ = 0.05, β = 0.05, δ = 0.40, ε = 0.50 and η = 0.0713, where the failure of suppressing self-excited vibration is shown.